The Catalytic Role of the Copper Ligand H172 of Peptidylglycine α-Hydroxylating Monooxygenase: A Kinetic Study of the H172A Mutant†

John P. Evans,‡,§ Ninian J. Blackburn,|| and Judith P. Klinman*,‡

Departments of Chemistry and Molecular and Cell Biology, University of California, Berkeley, California 94720-1460, and Department of Biochemistry and Molecular Biology, OGI School of Science and Engineering at OHSU, 20000 NW Walker Road, Beaverton, Oregon 97006-8921

Received August 23, 2006; Revised Manuscript Received October 9, 2006

ABSTRACT: An essential histidine ligand to the electron transfer copper (Cu_H) of peptidylglycine α-hydroxylating monooxygenase (PHMcc) was mutated to an alanine and found to retain copper binding and hydroxylase activity [Jaron, S., et al. (2002) *Biochemistry 41,* 13274−13282]. An extensive kinetic and deuterium isotope effect study finds this mutant to maintain full coupling of O_2 consumed to product formed despite a 3 order-of-magnitude decrease in k_{cat} and a 300-fold decrease in $k_{cat}/K_m(O_2)$. Unexpectedly, electron transfer is not rate-limiting in H172A. Rather, the increased kinetic isotope effect (KIE) on k_{cat} of 3.27 ± 0.39 suggests that C−H bond cleavage has become more rate-limiting, implicating a role for His^{172} that goes beyond that of a simple ligand to Cu_H. The mechanistic implications are discussed.

Peptidylglycine α-hydroxylating monooxygenase (PHM)[1] is a copper, ascorbate, and dioxygen-dependent enzyme that catalyzes the first step leading to the C-terminal amidation of glycine-extended peptides (Scheme 1) (*1*, *2*). It has both structural and catalytic similarities to the noncoupled binuclear copper protein, dopamine *β*-monooxygenase (D*β*M). The reaction involves a two-electron reductive cleavage of dioxygen with insertion of one oxygen atom into substrate and the formation of water and is catalyzed by a unique two-copper active site (Figure 1). Intriguing mechanistic questions remain regarding the O_2 species responsible for C−H abstraction; inherent to this question is the elucidation of the step in the mechanism in which the electron is transferred between the copper sites as well as the pathway through which the electron travels.

The two copper atoms alone supply the reducing equivalents required for the hydroxylation reaction; enzyme pre-reduced by a stoichiometric amount of ascorbate produces Cu^{2+} and product in a 2:1 ratio (*3*, *4*). The lack of any magnetic interactions by EPR suggests that the coppers do not form a binuclear center. Instead, the hydroxylation reaction is catalyzed at the Cu_M site through a hydrogen atom abstraction radical mechanism (*5*−*8*), with the other Cu site Cu_H supplying the additional electron by a long-range (∼11 Å), intramolecular electron transfer. The pathway for electron transfer between the copper sites has been unclear. A number of mechanisms have been proposed, including (i) a superoxide channeling mechanism whereby O_2 initially binds and is reduced at the Cu_H site and then channels to the Cu_M site as protonated superoxide (*9*, *10*), (ii) a substrate-mediated electron transfer pathway where a $Cu_M^{1+}(O_2^{\bullet-})$ abstracts the hydrogen atom (*11*, *12*), (iii) a mechanism where the roles of the coppers are reversed, such that substrate migration into the cavity separating the coppers facilitates hydroxylation at the Cu_H site (*13*), and (iv) a concerted hydrogen atom abstraction and electron transfer mechanism in which the second electron is transferred through an aci-carboxylate substrate intermediate coordinated to the Cu_H site via a swinging motion (*14*).

In previous studies with D*β*M, we have shown that a highly reduced O_2 species is an unlikely intermediate in the mechanism of hydrogen atom abstraction (*15*). No Cu^{2+} EPR signal was detected after the reduced protein was mixed with O_2 and an unreactive substrate analogue *β*,*β*-difluorophenethylamine. There are two possibilities for this observation: either the coppers remain in a Cu^{1+} prior to hydrogen atom abstraction or the diamagnetic Cu_M^{2+}−superoxo intermediate is formed. Most significantly, O_2 consumption was fully coupled to product formation, despite a large decrease in substrate reactivity such that hydrogen atom abstraction is fully rate-limiting. Thus, a steady-state accumulation of the activated dioxygen species produced no detectable leakage of reactive O_2 intermediates. The available data suggest the production of a low level of a $Cu_M^{2+}(O_2^{\bullet-})$ species which abstracts the hydrogen atom from substrate. This new mechanism invokes a one-electron transfer from Cu_M to dioxygen before hydrogen atom abstraction, followed by a solvent-mediated electron transfer from the Cu_M site (*16*).

† This work was supported by National Institutes of Health Grants GM39296 and GM25765 (to J.P.K.) and GM R01-NS27583 (to N.J.B.).

* To whom correspondence should be addressed. Tel: 510-642-2668. Fax: 510-643-6232. E-mail: klinman@berkeley.edu.

‡ University of California.

§ Present address: Department of Pharmaceutical Chemistry, University of California, San Francisco, Genentech Hall, 600 16th St., San Francisco, CA 94143-2280.

|| OGI School of Science and Engineering at OHSU.

[1] Abbreviations: PHM, peptidylglycine α-hydroxylating monooxygenase; PAM, peptidylglycine α-amidating monooxygenase; D*β*M, dopamine *β*-monooxygenase; PHMcc, peptidylglycine α-hydroxylating monooxygenase catalytic core consisting of amino acids 42−356 of rat PAM-1; EXAFS, extended X-ray absorption fine structure; PCA, protocatechuic acid; PCD, protocatechuate dioxygenase; MES, 2-(*N*-morpholino)ethanesulfonic acid.

10.1021/bi061734c CCC: $33.50
Published on Web 12/06/2006

Scheme 1: Reactions Leading to α-Amidated Peptide, Catalyzed by PHM and PAL[a]

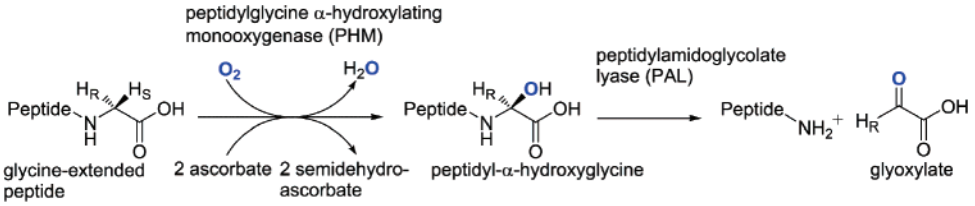

[a] These enzymes are often linked in a bifunctional form designated peptidylglycine α-amidating monooxygenase (PAM).

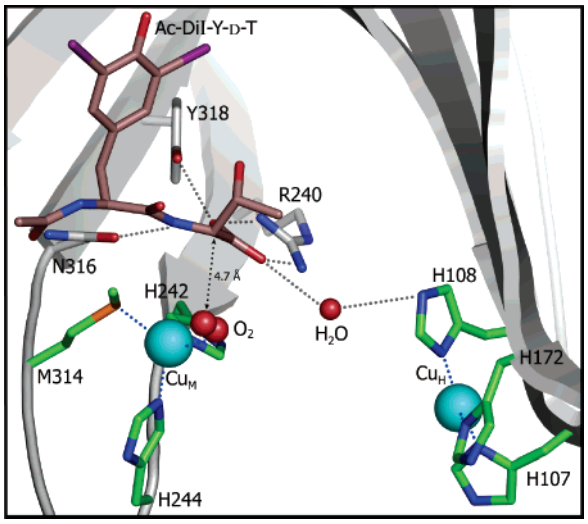

FIGURE 1: Precatalytic complex of PHMcc with bound peptide and dioxygen (adapted from ref *12*). Dioxygen is bound at the Cu_M site on the left, which has two His ligands and a Met ligand, while Cu_H, on the right, has three His ligands. The terminal oxygen atom of the $Cu_M(O_2)$ complex is 4.7 Å from the α-carbon which undergoes abstraction of the *pro-S* hydrogen atom. Rotation about the copper−oxygen bond could reduce this to ca. 3.3 Å. In this study, His^{172} has been mutated to an Ala residue.

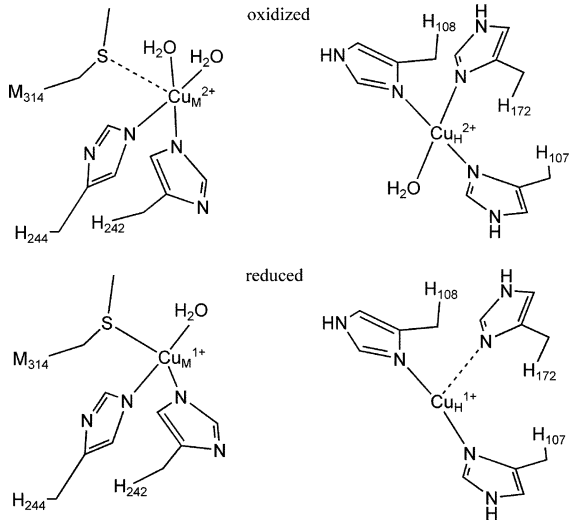

FIGURE 2: Coordination environment of oxidized (top) and reduced (bottom) PHM as deduced from EXAFS. The dotted lines represent ligands that are undetectable by EXAFS (>2.4 Å). In the oxidized structure, Cu_H (top right) is depicted as square planar, with H107, H108, H172, and a water as equatorial ligands; Cu_M (top left) is depicted as square pyramidal with H242, H244, and two waters as equatorial ligands and the long bond to M314 as the axial ligand. In the reduced structure, Cu_H (bottom right) is depicted as T-shaped with H107 and H108 ligands approximately trans along with a long bond to H172; Cu_M (bottom left) is depicted as tetrahedral with H242, H244, M314, and a water as ligands.

More recent results have supported a $Cu^{2+}(O_2^{\bullet-})$ mechanism in PHM. A crystallographic study of reduced PHMcc crystals soaked with a poor substrate, *N*-acetyldiiodotyrosyl-D-threonine (IYT), in which the *pro-S* hydrogen is difficult to cleave, has revealed a Cu_M coordinated to O_2 (*12*) (Figure 1). The oxygen is bound in an end-on fashion, at the Cu_M, presumably as a $Cu_M^{2+}(O_2^{\bullet-})$ (O−O distance of 1.23 Å), although the electron density is ambiguous and can also be assigned as $Cu_M^{1+}(O_2)$. A computational study used density functional theory to calculate the thermodynamics and kinetics of formation of two possible activated copper−dioxygen intermediates, $Cu^{2+}(OOH^-)$ and $Cu^{2+}(O_2^{\bullet-})$, as well as their ability to abstract a hydrogen atom from substrate (*17*). This study found that the hydrogen atom abstraction by the $1e^-$-reduced dioxygen species is thermodynamically and kinetically more favorable than by the $2e^-$-reduced dioxygen species.

The crystallographic and spectroscopic data have not always agreed. Large changes in the coordination environments of the copper sites have been observed by extended X-ray absorption fine structure (EXAFS) studies on PHM and are not observed in X-ray crystallography. This has led to a different proposal for the electron transfer mechanism (*18*). The spectroscopically determined coordination environments of the copper centers for the oxidized and reduced forms of PHM are shown in Figure 2. Reduction changes the Cu_H center from four-coordinate tetrahedral to two-coordinate planar and leads to loss of its solvating water ligand. Additionally, one of its histidine ligands (H172) becomes undetectable by EXAFS. In contrast, X-ray crystallography shows the Cu_H site maintaining a three-coordinate geometry, but with tighter ligation by His^{172} to the reduced Cu (*11*). The Cu_M center remains four-coordinate, losing water and gaining a long bond to methionine. By crystallography, the Cu_M site remains four-coordinate tetrahedral, with no changes in the position of M314 and only small changes in the position of the water ligand. The large structural changes at the metal sites revealed by EXAFS have been invoked to rule out a rapid electron transfer between the sites and, together with FTIR evidence for substrate-induced CO binding to the Cu_H site, led to the earlier proposal of the superoxide channeling mechanism (*9*).

EXAFS spectroscopic characterization of the H172A mutant of PHM showed little disruption of copper binding, yet activity was decreased over 300-fold from WT (*10*). The oxidized and reduced mutant enzyme showed few structural changes at the Cu_H site; in the oxidized structure a water molecule is recruited in place of the histidine, and in the reduced structure Cu_H becomes truly two-coordinate. If H172 is not essential for copper binding, the substantial decrease in rate suggests another important role. Thus, H172 was

proposed to act as an active site acid catalyst, protonating the resulting superoxide ion (*10*).

In the present work, a detailed analysis of the role of H172 in the mechanism of PHM was investigated through extensive kinetic and isotope effect studies on the H172A mutant form of the enzyme. The kinetic parameters for WT and H172A were determined using the alternate electron donor, potassium ferrocyanide. These parameters are decreased significantly in the mutant, with a 3000-fold decrease in k_{cat} and a 300-fold decrease in $k_{cat}/K_m(O_2)$. This indicates that mutation of histidine 172 to alanine significantly affects O_2 binding and substrate hydroxylation at the Cu_M site. The deuterium kinetic isotope effects for H172A of 3.27 ± 0.39 and 2.75 ± 0.79 on k_{cat} and $k_{cat}/K_m(O_2)$, respectively, clearly indicate that electron transfer has not become fully rate-limiting and that hydrogen atom transfer is equally rate-determining for both parameters. The possible impact of H172A on the reaction mechanism is discussed in the context of these new results.

MATERIALS AND METHODS

Materials. *N*-Benzoylglycine (hippuric acid), sodium ascorbate, protocatechuic acid (PCA), protocatechuate dioxygenase (PCD), and 2-(*N*-morpholino)ethanesulfonic acid (MES) were purchased from Sigma. Catalase (65000 units/mg) in the form of a suspension was from Roche Molecular Biochemicals. α-Hydroxyhippuric acid was purchased from Aldrich and used without further purification. *N*-Benzoyl-[2-$^2H_2$]glycine (dideuterated hippuric acid) was synthesized from commercially available [2-$^2H_2$]glycine (98% ^2H; Cambridge Isotope Laboratories, Inc.) as previously described (*19*).

Enzyme Preparation and Purification. The Chinese hamster ovary cell line used to express wild-type and H172A PHMcc protein was constructed as described previously (*20*). Protein concentration was determined using the absorbance at 280 nm, $\epsilon = 0.98$ for a 1 mg/mL solution (*9*). H172A was purified as described previously (*10*, *13*).

Copper Reconstitution. Trace metal analysis of enzyme-bound copper was performed on a Perkin-Elmer 3000DV inductively coupled plasma atomic emission spectrophotometer using commercially available metal standard solutions. As isolated following purification, H172A contained less than 0.3 Cu/protein. The enzyme was reconstituted following the procedure described (*21*) to obtain H172A containing 1.4 Cu/protein. A 10 kDa membrane Biomax Millipore ultrafree centrifugal filtration device was washed with 4 mL of 50 mM potassium phosphate, pH 7.4, to remove preservatives (spun at 2000 rpm for 30 min). In the example described here, a 1 mL solution of 10.87 mg/mL H172A PHMcc was diluted with 3 mL of 50 mM potassium phosphate, pH 7.4, and the solution was spun at 2000 rpm for 40 min to concentrate the solution down to 1 mL. This step was repeated two more times. To the washed 1 mL of enzyme solution (311 μM) was added 3 mL of 234 μM $CuSO_4$ and 50 mM potassium phosphate, pH 7.4, such that the final copper to protein concentration was in a 2:1 ratio. The sample was incubated on ice for 10 min and then concentrated to 1 mL. Another 3 mL of 5 μM $CuSO_4$ and 50 mM potassium phosphate, pH 7.4, was added and subsequently concentrated to a final volume of 850 μL. Aliquots of 60 μL were frozen with liquid N_2 and placed in the −80 °C freezer until further use.

Stoichiometry Assays. These experiments were performed in two steps. First, the decrease in oxygen concentration was measured with a YSI model 5300 biological oxygen monitor following addition of either WT or mutant PHMcc to a final assay volume of 1 mL at 37 °C. Assay conditions consisted of 100 mM MES, pH 6.0, 30 mM KCl, 10 mM hippuric acid, and either 0.2 mM potassium ferrocyanide or 10 mM sodium ascorbate for reductant. Assays with ascorbate also contained 100 μg/mL catalase (*22*). A concentration of dissolved O_2 for these assay conditions was determined to be 209 μM by the PCA/PCD assay, as described previously (*23*). Briefly, the full amplitude of oxygen uptake was recorded following the addition of PCA to an assay mixture containing 100 mM MES, pH 6.0, 30 mM KCl, and an excess of PCD. Assays with WT PHM and ascorbate required less than 3 min, while mutant reactions with ferrocyanide required 9 min for approximately 8 μM O_2 to be consumed, at which time 100 μL of 1 M $HClO_4$ was added to fully quench the reaction. Samples were stored at −80 °C until further analysis by HPLC to determine the amount of product formed as described below.

HPLC Conditions To Separate Hippuric Acid from α*-Hydroxyhippuric Acid.* Frozen samples stored at −80 °C were thawed and centrifuged for 10 min immediately before HPLC analysis. A Beckman Ultrasphere C18-IP 5 μm column (4.6 × 250 mm) with a guard column (4.6 × 7.5 mm) was equilibrated with 1% CH_3CN in 50 mM ammonium acetate, pH 5.5 (buffer A). A volume of 50 μL of the quenched sample was injected. The column was washed for 30 min with buffer A, followed by a 10 min gradient to 10% CH_3CN in 50 mM ammonium acetate, pH 5.5 (buffer B). The column was washed for 5 min with buffer B, returned to buffer A over 5 min, and then allowed to reequilibrate for 10 min prior to the next injection. The compounds eluting, α-hydroxyhippuric acid (14 min) and hippuric acid (28 min), were detected at 230 and 280 nm. No benzamide was detected in experiments with PHMcc. The lack of benzamide is consistent with model studies of carboxamide dealkylation at pH 6 (*24*, *25*). The integrated peak area was compared to a standard curve of mock-quenched assays. Blanks, in which no enzyme was added, were used to determine the amount of contaminant eluting with the same retention time as product and were subtracted from each assay.

α*-Hydroxyhippuric Acid Standard Curve.* Using commercially available α-hydroxyhippuric acid, mock-quenched assay mixtures including quencher were constructed, with concentrations of α-hydroxyhippuric acid ranging from 0.05 to 2 nmol.

Steady-State Assays and Noncompetitive Kinetic Isotope Effects. Initial rates were measured from the rate of oxygen consumption at varied oxygen and protiated or dideuterated hippuric acid concentrations. The decrease in oxygen concentration was measured with a YSI model 5300 biological oxygen monitor. The temperature of the chamber was maintained at 37.0 ± 0.1 °C with a Neslab circulating water bath. Reaction mixtures (1 mL) contained 100 mM MES (pH 6.0), 30 mM KCl, 1 μM $CuSO_4$, 0.4 mM $K_4Fe(CN)_6$, and various amounts of hippuric acid substrate (1.3−40 mM) at a range of concentrations of dissolved oxygen (0.03−0.96 mM). Concentrated solutions of $K_4Fe(CN)_6$ and $CuSO_4$ were

made fresh and kept on ice. The oxygen concentration was varied by stirring the reaction mixtures for 4 min with premixed O_2/N_2 mixtures in the appropriate proportions to yield the desired O_2 concentration. The resulting oxygen concentration was determined from the known concentration of dissolved oxygen in air-saturated water (217 μM at 37 °C) and O_2-saturated water (1043 μM at 37 °C). Reactions were initiated by the addition of enzyme (2−8 μL). Velocities of both unlabeled and dideuterated substrates at a given concentration were obtained in a single experiment using the same stocks of the other reaction components to minimize fluctuations in experimental conditions. The initial velocity data obtained by varying the concentration of one substrate at a fixed concentration of the second substrate were fit to eq 1 using the program Kaleidagraph (Synergy Software):

$$v = \frac{VS}{K + S} \quad (1)$$

where V is the maximal velocity, S is the substrate concentration, and K is the Michaelis constant. In the case of noncompetitive substrate self-inhibition, data were best fit to the equation:

$$v = \frac{VS}{K + S(1 + S/K_i)} \quad (2)$$

where K_i is the substrate inhibition constant.

To determine the kinetic mechanism from the series of experiments where the concentration of hippuric acid was varied at multiple concentrations of O_2, the data were fit by nonlinear least-squares regression using the program Mathematica (Wolfram Research) to eqs 3 and 4 describing an equilibrium-ordered mechanism and a two-substrate steady-state mechanism, respectively (*26*):

$$v = \frac{VAB}{K_{ia}K_b + K_bA + AB} \quad (3)$$

$$v = \frac{VAB}{K_{ia}K_b + K_bA + K_aB + AB} \quad (4)$$

where A and B are the hippuric acid and O_2 concentrations, respectively, V is the maximal velocity, K_a and K_b are the Michaelis constants for A and B, respectively, and K_{ia} is the dissociation constant of A.

RESULTS

Coupling of Oxygen and Substrate Consumption. An interesting feature of H172A is that it maintains copper binding near WT levels, as well as hydroxylating activity, despite the loss of this important copper ligand (*10*). Under the standard assay conditions, 10 mM hippuric acid and air-saturated buffer, H172A shows a 1000-fold decrease in turnover rate. One consequence of this lower rate is that a considerable amount of enzyme (final concentration of 2 μM, equivalent to 0.07 mg/mL protein) is required for each assay. Assays were initially performed with the in vivo electron donor ascorbate since activity assays for wild-type PHM are routinely carried out with this reductant for maximal activity. A side effect of using ascorbate is that hydrogen peroxide is produced through ascorbate and transition metal catalyzed autoxidation reactions (*27*, *28*). Hydrogen peroxide inactivates PHM through an as yet unknown mechanism, and catalase is normally added to the assays as a peroxide scavenger (*22*). One potential complication for the stoichiometry experiments is oxygen evolution in the catalase reaction, which could interfere with the oxygen consumption measurement if large amounts of H_2O_2 were produced. Therefore, catalase was omitted from the assays.

A second complication is that the background rate of ascorbate oxidation is dependent on the concentration of free Cu^{2+}, varying from 0.5 nmol of O_2 min^{-1} with no exogenous Cu^{2+} up to 3 nmol of O_2 min^{-1} with 4 μM exogenous Cu^{2+}. Since the dissociation constants of copper for H172A are unknown, it was not possible to estimate the amount of free copper in solution. Wild-type PHMcc has an estimated K_D for copper of 0.06−0.1 μM (*13*, *29*). The large background rates of O_2 consumption catalyzed by ascorbate and copper autoxidation were not conducive to measuring accurate quantities of oxygen consumed with the mutant. Also, because of the copper ion dependence of the ascorbate-catalyzed autoxidation, addition of large quantities of enzyme (2 μM range) would be expected to increase the ascorbate background rate. In fact, coupling ratios of dioxygen consumed to product formed, using ascorbate as the reductant, varied from 1.69 ± 0.22 when the enzyme is preincubated with copper (1.4−1.8 Cu/enzyme) to 0.84 ± 0.01 for the as-purified enzyme (containing 0.2 Cu/enzyme). Presumably the ratio greater than 1 is from metal ions dissociating from the enzyme and reacting with ascorbate during the assay. In this manner the initial ascorbate background rate will be underestimated and produce an overestimate of the amount of oxygen consumed to product formed.

An alternate reducing agent, lacking the high background and metal ion dependent O_2 consumption, was sought. Ferrocyanide has been shown to be an effective reducing agent for the analogous enzyme DβM (*30*) and has been tested with PAM (*31*). Furthermore, the background rate with ferrocyanide is independent of copper. Therefore, we decided to use ferrocyanide as the reductant in all further studies. Background rates with ferrocyanide were negligible and depended largely on the quality of the electrode used. Since autoxidation with this reductant is not a problem, it was possible to omit catalase from the assays without concern for PHM inactivation.

Oxygen consumption was measured over a period of minutes with an oxygen electrode, with the background rate measured for at least 3 min prior to adding enzyme (see Figure 3). At the appropriate reaction times, assays were acid-quenched, and the amount of hydroxylated product (α-hydroxyhippuric acid) was determined by applying an aliquot of the quenched assay to the HPLC and comparing to a standard curve.

Wild-type PHM gave a ratio of oxygen consumed to hydroxylated product formed (coupling ratio) of 0.90 ± 0.08 with ascorbate as the electron donor and 0.86 ± 0.13 when using $K_4Fe(CN)_6$ (see Table 1). H172A shows a coupling ratio of 0.93 ± 0.12, with ferrocyanide as the reductant. Since these values are unity, within error, it is possible to conclude that there is full coupling of oxygen consumption to hydroxylated product formation in H172A. We note that since the coupling ratios measured with ferrocyanide or with ascorbate and very low amounts of copper/enzyme are similar

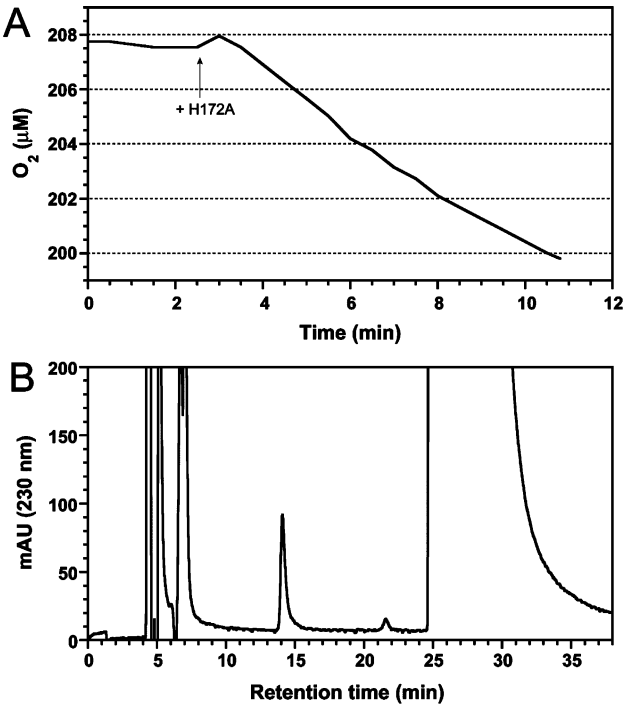

FIGURE 3: Discontinuous assay for H172A to compare the O_2 consumed (A) with product formed (B). α-Hydroxyhippuric acid elutes at approximately 14 min, and hippuric acid elutes at 28 min. All other assay components elute in the dead time centered at 6 min.

Table 1: Stoichiometry of O_2 Consumed to Product Formed

enzyme form	reductant	average [PHM] (μM)	O_2/product
WT	ascorbate	0.03	0.90 ± 0.08
WT	ferrocyanide	0.01	0.86 ± 0.13
H172A	ferrocyanide	2.23	0.93 ± 0.12

and close to unity, the higher values, obtained in the presence of ascorbate and higher copper/enzyme concentrations, can be attributed to increased background rate of ascorbate air oxidation following dissociation of copper from the mutant enzyme.

Possible reasons why the observed uncoupling ratios tend to cluster somewhat below unity could be (i) overestimation of the observed background rate of oxygen consumption and/or (ii) contamination of the commercially available α-hydroxyhippuric acid used to produce the standard curve (although no impurities other than up to 0.2% benzamide were detected).

Steady-State Kinetics and Isotope Effects. The Cu_H site in H172A might be expected to show different electron transfer properties than WT. To investigate its catalytic mechanism further, an extensive kinetic analysis to measure k_{cat}, k_{cat}/K_m, and the isotope effects on these parameters for WT and H172A was undertaken using the alternate reductant potassium ferrocyanide. Hippuric acid was used as the substrate since it is readily available and has been used in previous kinetic studies on PHMcc where ascorbate was used as the reductant (*19*). The initial velocities were measured as a function of dioxygen and protiated and dideuterated hippuric acid. The isotope effects on these parameters can provide information on the order of addition of reactants as well as the location and degree of rate limitation of the

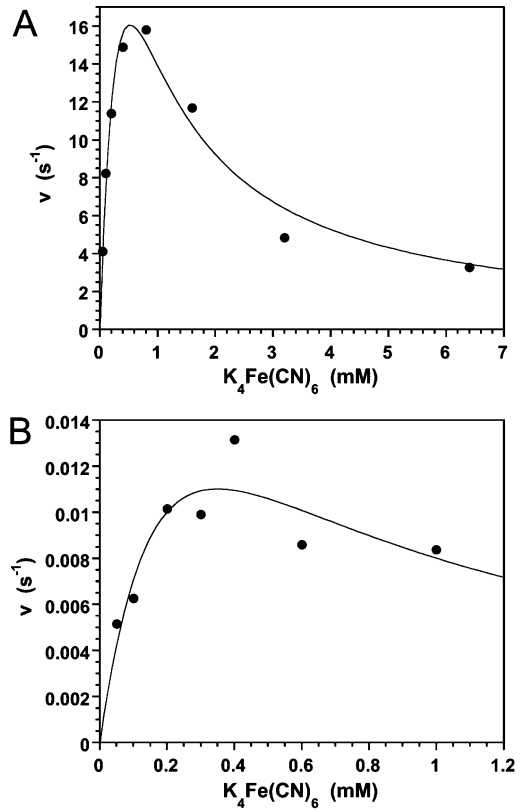

FIGURE 4: Inhibition of WT (A) and H172A (B) by the one-electron reductant potassium ferrocyanide. For WT (40 mM HA and 0.95 mM O_2), fitting to eq 2 results in $V_{max} = 55$ s^{-1}, $K_m = 0.6$ mM, and $K_i = 0.4$ mM. For H172A (40 mM HA and 0.21 mM O_2), $V_{max} = 0.029$ s^{-1}, $K_m = 0.3$ mM, and $K_i = 0.4$ mM.

isotope-sensitive step (*32*). Comparison of these parameters for wild type to those of the mutant gives information on the location in the kinetic mechanism of the large decrease in rate and allows for a better understanding of the role of H172 and how its absence affects the mechanism.

Ferrocyanide Inhibition and the Correction. As presented in Figure 4, rates at high concentrations of ferrocyanide are decreased, characteristic of substrate inhibition, presumably from cyanide anion binding to and removing copper from the enzyme. Under the standard assay conditions, using 1 μM exogenous Cu added to the assays, wild-type and mutant PHMcc were inhibited by ferrocyanide at concentrations above 0.6 and 0.4 mM, respectively (see Figure 4). Increasing the exogenous copper concentration up 10 μM (at 0.4 mM ferrocyanide) had no beneficial effect on activity (data not shown). Therefore, a constant concentration of 0.4 mM ferrocyanide and 1 μM exogenous copper was chosen for the steady-state assays in which substrates hippuric acid and dioxygen were varied. However, this concentration of ferrocyanide was not fully saturating.

To avoid kinetic ambiguities arising from the half-reaction in which the copper sites are reduced, it is desirable to fully saturate with the reductant, ferrocyanide. Experiments in which ferrocyanide was varied at constant hippuric acid and O_2 concentrations showed ferrocyanide K_m's for WT PHM to vary from 0.03 mM at low HA and O_2 (4 mM HA, 0.21 mM O_2) to 0.26 mM at high concentrations of HA and O_2 (40 mM HA, 0.95 mM O_2; data not shown). Deuterated hippuric acid showed a similar trend, with ferrocyanide K_m's ranging from 0.10 mM at low HA and O_2 to 0.21 mM at

Table 2: Steady-State Kinetic Parameters for WT and H172A PHMcc with 0.4 mM Ferrocyanide

	wild type[a]			H172A[b]		
parameter	[$^1H_2$]HA	[$^2H_2$]HA	KIE	[$^1H_2$]HA	[$^2H_2$]HA	KIE
k_{cat} (s^{-1})	51 (3)	35 (3)	1.45 (0.15)	0.022 (0.001)	0.0068 (0.0007)	3.27 (0.39)
k_{cat}/K_m(HA) ($mM^{-1}\,s^{-1}$)	NA[c]	NA	NA	0.0053 (0.0008)	0.0030 (0.0009)	1.77 (0.63)
$k_{cat}/K_m(O_2)$ ($mM^{-1}\,s^{-1}$)	176 (39)	80 (18)	2.20 (0.70)	0.422 (0.058)	0.154 (0.039)	2.75 (0.79)
$K_m(O_2)$	0.292 (0.063)	0.442 (0.094)		0.053 (0.010)	0.044 (0.015)	

[a] Kinetic parameters were obtained by fitting data to the equation describing an equilibrium-ordered mechanism (eq 3). [b] Kinetic parameters were obtained by fitting data to the equation describing a two-substrate steady-state mechanism (eq 4). [c] NA = not available.

high HA and O_2. However, mutant PHM showed a rather different trend. Upon varying ferrocyanide at multiple constant concentrations of HA and O_2, ferrocyanide K_m's ranged from 0.12 mM at low substrate concentration to 0.14 mM at high concentration for protiated hippuric acid and a constant K_m of 0.05 mM for dideuterated hipurric acid. Therefore, to apply a correction, the observed rates at 0.4 mM ferrocyanide were compared to the extrapolated rates at fully saturating ferrocyanide, and the difference between the two was plotted as a function of hippuric acid and dioxygen. A correction was then applied to each rate based on the hippuric acid and dioxygen concentrations.

The limiting parameters of k_{cat}, k_{cat}/K_m(HA), and $k_{cat}/K_m(O_2)$ along with the deuterium kinetic isotope effects on these parameters for WT and H172A PHM using ferrocyanide as reductant are summarized in Table 2. At a concentration of 0.4 mM potassium ferrocyanide, protiated and dideuterated hippuric acid concentrations were first varied while maintaining a constant O_2 concentration. This analysis produced apparent V_{max} and V_{max}/K_m(HA) values, which were then replotted versus [O_2] to give the extrapolated parameters k_{cat}, $k_{cat}/K_m(O_2)$, and k_{cat}/K_m(HA) at infinite concentrations of both substrates (see Figure 5). It is interesting to note that the kinetics of WT with different reductants, 0.4 mM ferrocyanide with the correction (this study) and 10 mM ascorbate (*19*), do not vary significantly. The corrected k_{cat} with ferrocyanide is 30% higher than that with ascorbate (39.1 ± 0.5 s^{-1}), yet the isotope effect on this parameter remains identical.

With 10 mM ascorbate, WT PHM proceeds through an equilibrium-ordered mechanism, with hippuric acid binding before O_2 (*19*). With ferrocyanide, data were fitted to the equations describing an equilibrium-ordered (eq 3) and a two-substrate steady-state mechanism (eq 4), with a slightly better fit to the equilibrium-ordered equation as determined by the statistical parameter σ, the square root of the residual least squares (*26*). The σ values for the fit to eqs 3 and 4 are 1.26 and 1.28, respectively, for the protiated hippuric acid data and 0.68 and 0.70, respectively, for the dideuterated hippuric acid data. In addition, the K_a (K_{HA}) values obtained when fitting the initial velocity data to the two-substrate steady-state equation (eq 4) are small with standard errors larger than the corresponding values, indicating a lack of significance for this term and suggestive of an equilibrium-ordered mechanism.

In an equilibrium-ordered mechanism, where hippuric acid is predicted to bind first, a constant isotope effect on k_{cat}/K_m(HA) would be observed that is independent of the concentration of O_2 and equal to the isotope effect on $k_{cat}/K_m(O_2)$ (*19*). From a plot of the apparent V_{max}/K_m(HA) versus O_2 concentration (not shown), very high and unreachable concentrations of O_2 were needed, up to 8 mM O_2, to get an accurate value of the limiting isotope effect on this parameter. However, a plot of apparent $^DV_{max}/K_m$(HA) versus O_2 concentration (Figure 6) provides an estimated value of 5, which is comparable to wild type with ascorbate (see Figure 1B in ref *19*). In the case of O_2, a $k_{cat}/K_m(O_2)$ with ferrocyanide is seen to be comparable to that with ascorbate, while the isotope effect is smaller (2.20 ± 0.70). This latter value indicates an inequality between $^DV_{max}/K_m$(HA) and $^DV_{max}/K_m(O_2)$, making the assignment of the kinetic mechanism for WT enzyme in the presence of ferrocyanide to equilibrium-ordered somewhat equivocal. The major consequence of fitting to an equilibrium-ordered mechanism is an inability to estimate k_{cat}/K_m(HA), with values for k_{cat} and $k_{cat}/K_m(O_2)$ and microscopic rate constants (Tables 2 and 3) within the error bounds of the same

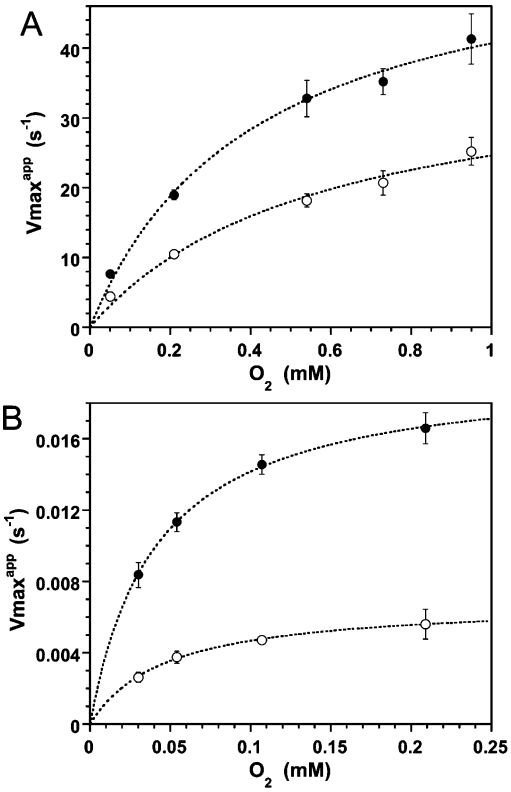

FIGURE 5: Replots of apparent V_{max} for saturating hippuric acid at varied, fixed concentrations of O_2 for WT (A) and H172A (B) PHMcc. Each point represents the apparent V_{max} measured by variation of [$^1H_2$]HA (●) or [$^2H_2$]HA (○) followed by least-squares fitting to the Michaelis−Menten equation; the error bars represent the standard error in the initial curve fit. The data shown here were fitted to a hyperbolic function, $y = ax/(b + x)$, to obtain the extrapolated k_{cat} values for WT, [$^1H_2$]HA 57 ± 5 s^{-1} and [$^2H_2$]HA 37 ± 6 s^{-1}, and for H172A, [$^1H_2$]HA 0.0206 ± 0.0006 s^{-1} and [$^2H_2$]HA 0.0067 ± 0.0001 s^{-1}.

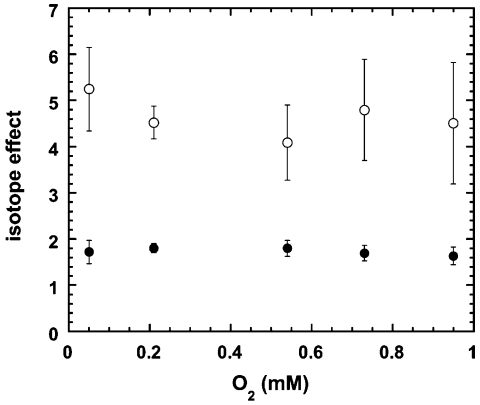

FIGURE 6: Dependence of apparent $^{D}V_{max}$ (●) and apparent $^{D}V_{max}/K_m$(HA) (○) on the concentration of dioxygen for WT PHM using ferrocyanide.

Table 3: Intrinsic Rate Constants for Wild-Type and H172A PHM According to Scheme 2

constant	wild type	H172A	wild type/ H172A
$k_{3\,O_2}$ ($mM^{-1}\,s^{-1}$) [a]	196 ± 53	0.496 ± 0.094	~400
$k_{4\,O_2}$ (s^{-1})[a]	(152 ± 221)[c]	(0.020 ± 0.044)[c]	
$k_{3\,HA}$ ($mM^{-1}\,s^{-1}$)[a]	NA	0.006 ± 0.001	
$k_{4\,HA}$ (s^{-1})[a]	NA	(0.008 ± 0.018)[c]	
k_5 (s^{-1})[a]	1330 ± 420	0.113 ± 0.020	~12000
k_7 (s^{-1})[a]	53 ± 4	0.027 ± 0.002	~2000
$K_{D\,O_2}$ (mM)[b]	0.77 ± 0.42	0.04 ± 0.02	
$K_{D\,HA}$ (mM)[b]		1.41 ± 1.0	

[a] Calculated from the equations derived in ref *52* (eqs 1−8, Table 6) using a value of 12.7 ± 1.0 for the intrinsic isotope effect as described in ref *19*. [b] Calculated using the equations derived in ref *56* (eq 2, Table 5). [c] These parameters are undetermined due to the large propagated errors.

parameters estimated using the steady-state assumption (data not shown).

The mutant data were obtained in a similar fashion to wild type (see Figure 5); in this case, they were found to fit better to the equation describing a two-substrate steady-state mechanism (eq 4). The σ values for the fit to eqs 3 and 4 are 0.0015 and 0.0010, respectively, for the protiated hippuric acid data and 0.00091 and 0.00075, respectively, for the dideuterated hippuric acid data. The first-order rate constant k_{cat}, reflecting all steps in the mechanism from formation of the ternary complex through product release, is significantly decreased from WT by almost 3000-fold and very surprisingly shows an elevated isotope effect (Table 2). At the same time the second-order rate constant $k_{cat}/K_m(O_2)$ shows a 300-fold decrease from WT. The trends in all of the parameters indicate that the measured activity is unlikely to arise from any WT contamination. The deuterium isotope effect on both k_{cat}/K_m(HA) and $k_{cat}/K_m(O_2)$ is characteristic of the steady-state-random kinetic mechanism shown in Scheme 2.

DISCUSSION

A detailed kinetic characterization of WT and H172A PHMcc, with the alternate reductant ferrocyanide, was undertaken in order to clarify the proposed mechanism for O_2 and C−H activation by the noncoupled binuclear copper monooxygenases (*15*), as well as the location of the mechanistic step involving intramolecular electron transfer from the Cu_H to Cu_M site. A change in the coordination

Scheme 2: PHM Kinetic Mechanism in Which Substrate and O_2 Bind in a Random Fashion

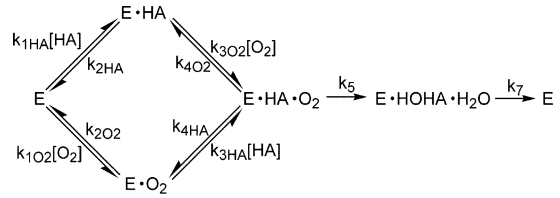

Scheme 3: Possible Cu/O_2 Species Capable of Hydrogen Atom Abstraction

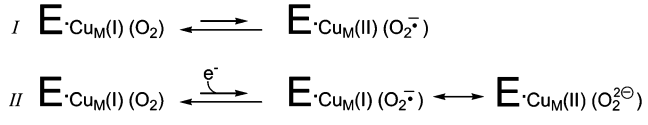

environment at the Cu_H site through site-directed mutagenesis could slow down the electron transfer step without affecting any other steps in the mechanism. In this way the two plausible mechanisms in which substrate binds and dioxygen is activated and reduced at the Cu_M site (Scheme 3) might be distinguished by a steady-state kinetic analysis. In fact, deletion of the Cu_H site altogether might provide information on the mechanism through a detection of Cu^{2+} intermediates, or activated O_2 and substrate intermediates produced through an unproductive turnover. Mechanisms have been proposed for PHM whereby hydroxylated product is formed prior to electron transfer from the Cu_H site (*15*−*17*). Removal of the Cu_H center to obtain the half-apoprotein is possible by dialyzing protein solution saturated with CO against cyanide where the CO binds to the Cu_M site and protects it from cyanide (*33*, *34*). However, the copper sites of PHM are labile, allowing for redistribution of copper on the time scale of steady-state activity assays, such that some enzyme becomes fully metallated.

The general requirement for the chemical mechanism of PHM and DβM is that C−H cleavage, the first irreversible step, must be connected to the activation of O_2 through a series of fully reversible steps (*15*, *35*, *36*). Possible activated oxygen species capable of hydrogen atom abstraction that meet this requirement include either a one-electron or two-electron reduced species (Scheme 3). The methionine ligand contributes to the stability of the reduced Cu_M site, having a much longer bond to the oxidized than to the reduced copper (*18*). In addition, formation of these intermediates is uphill in free energy, and equilibrium is expected to lie far to the left (*15*, *17*). In I, a $Cu_M^{2+}(O_2^{\bullet-})$ catalyzes C−H abstraction, with the second electron being transferred after the first irreversible step (C−H abstraction). In the simplest case, a decreased electron transfer rate for mutant versus WT would only appear in the k_{cat} term, while $k_{cat}/K_m(O_2)$ would remain unchanged since this second-order rate constant is independent of step(s) after k_5 (Scheme 2). For a mechanism in which the second electron is transferred from Cu_H reversibly, prior to C−H abstraction (II in Scheme 3), both k_{cat} and $k_{cat}/K_m(O_2)$ would decrease by roughly the same amount.

A distinct advantage of the PHM system over DβM is that it can be isolated from a relatively high level expression system which facilitates site-directed mutagenesis experiments (*20*, *37*, *38*). The expressed PHMcc is small (35 kDa) and has allowed for crystallographic characterization of multiple forms of the enzyme, including the oxidized (*39*),

oxidized with bound substrate, reduced (*11*), and reduced with bound substrate and dioxygen (*12*). Initial site-directed mutagenesis experiments, in which the conserved histidine ligands to the Cu_M and Cu_H sites were each mutated to alanines, resulted in a lack of catalytic activity (*37*, *38*) with no alteration in the rate of secretion of the mutant proteins (*37*); this indicated that the His residues, although essential for catalytic activity, were not essential for the folding of newly synthesized PHMcc into a secretable form. These activity assays at the time were not sensitive enough to detect the residual activity of the H172A mutant.

Closer examination of H172A found that activity was retained, although decreased by >300 fold with the substrate Ac-YVG (*10*). Interestingly, this mutant still binds Cu^{2+}, even though His^{172} coordinates more closely to and is an important ligand to the oxidized copper (see Figure 2). The extent of copper binding to reconstituted H172A was found to be identical to wild type, with a 1.4:1 copper to protein ratio. Another ligand involved in redox-based coordination changes is the methionine at the Cu_M site, which coordinates more closely to the reduced copper. Mutation of Met314 to Ile eliminates metal binding at the reduced Cu_M site (*18*, *40*). The mechanism whereby H172A would affect the reduction potential at the Cu_H site is likely to be a combination of the reduced electron-donating property of Ala, as well as a change in the ligand reorganization properties as the metal cycles between the +1 and +2 valence states.

PHM is primarily localized within secretory vesicles, a compartment of the cell that contains high levels of ascorbate. Therefore, the enzyme might be expected to maintain tight coupling of O_2 binding and reduction with substrate binding and oxidation, to prevent deleterious reactive oxygen from propagating out of control. This contrasts with other hydroxylating enzymes such as phenylalanine hydroxylase and cytochrome P450, which show uncoupling of oxygen consumption from product formation in assays where substrate analogues are used (*41*, *42*), or when mutations to important active site residues disrupt substrate or cofactor binding (*43*−*46*). Various modes of uncoupling can be achieved, including a two-electron "oxidase" uncoupling where hydrogen peroxide is produced or a four-electron "oxygenase" form of uncoupling where water is produced. In PHM, a four-electron uncoupling pathway is unlikely since the enzyme reacts with reductant in a separate half-reaction. O_2 activation that proceeds through a superoxide channeling mechanism or formation of a $Cu(I)(O_2^{\bullet-})$ (II in Scheme 3) might lose superoxide and lead to an unproductive turnover. However, none of these side products are formed in H172A PHMcc, as a tight ratio of oxygen consumption to product formation is observed (Table 1). It is remarkable that H172A PHM has maintained tight coupling despite a significant decrease in rate. Full coupling rules out the superoxide channeling mechanism and suggests that H172A has not drastically altered the basic characteristics of the O_2 binding and activation pathway.

Ferrocyanide was chosen as the primary reductant in these studies instead of ascorbate. With DβM, a full examination of kinetic parameters with ferrocyanide has indicated that it is nearly as competent as ascorbate (*30*). Ascorbate and ferrocyanide show similar reduction potentials; ferrocyanide is 0.36 V while ascorbate has a one-electron reduction potential of 0.39−0.42 V (*47*, *48*). In addition, molecular modeling studies suggest that ferrocyanide and ascorbate possess similarities in possible binding interactions at the binding site on the protein, the location of which is unknown. In PAM, the one electron donor, ferrocyanide was found to stimulate amidation of D-Tyr-Val-Gly, although with an efficiency approximately 40% of that of ascorbate (*31*); however, only one concentration of ferrocyanide was used, 2 mM, with 1 μM exogenous copper, so inhibition was not discussed. In DβM, intersecting kinetic patterns were observed by Lineweaver−Burk analysis, when ferrocyanide was used as a reductant (*49*). This phenomenon was attributed to substrate inhibition (*50*), likely due to free cyanide that could be overcome by added copper (*30*, *51*). In the present studies, ferrocyanide is found to be as competent a reductant as ascorbate; however, the inhibition at higher concentrations was not eliminated with added copper.

Comparing the rates of protiated and dideuterated hippuric acid with ferrocyanide for WT and H172A, k_{cat} and $k_{cat}/K_m(O_2)$ for H172A decrease significantly, while the deuterium isotope effects on these parameters unexpectedly increase. It was thought that steps in the mechanism affected by the mutation would only involve those in which the Cu_H site was involved, since substrate and O_2 binding appear restricted to the Cu_M site. However, the C−H abstraction step has become more rate-limiting in the mutant, negating the hypothesis that H172A would solely affect the electron transfer rate.

The intrinsic rate constants for the kinetic mechanism shown in Scheme 2 can be calculated from the measured kinetic parameters, their isotope effects, and the intrinsic isotope effect. This methodology has been used previously in calculating the rate constants for the reactions catalyzed by DβM (*52*), WT PHM (*19*), and Y318F PHM (*36*). Although the intrinsic isotope effect for H172A is not available, a previously determined intrinsic isotope effect for WT enzyme which is identical to DβM (*53*) should serve as a rough guide to determine the steps in the mechanism most affected by the mutation (Table 3). It can be seen that the H172A mutation most notably alters k_5: an approximate 12000-fold decrease is seen in the rate of the C−H bond cleavage step. The rate constant $k_{3\,O_2}$, corresponding to the rate of association of O_2 to the E·HA binary complex, is the least affected, being decreased by approximately 400-fold.

There are multiple explanations to account for the unexpectedly large changes in the chemical step by H172A. First, mutation may have conferred nonspecific structural changes that propagate throughout the protein, creating an inactive form that is in equilibrium with the active form. As a first approximation, this would predict that all rate constants would be similarly affected with unchanged isotope effects, with the portion of the enzyme that is active and in the correct configuration for catalysis behaving the same as wild type. However, examination of Table 3 indicates differential effects on the rate constants, leading to a k_{cat} that is diminished ~10-fold more than $k_{cat}/K_m(O_2)$, relative to wild type. As discussed earlier, mechanism I in Scheme 3 [where a $Cu_M^{2+}(O_2^{\bullet-})$ catalyzes C−H abstraction] places the other possible rate-limiting steps in the mechanism, such as intramolecular electron transfer and product release, in k_{cat}. This mechanism could account for the altered redox properties of the Cu_H site affecting k_{cat} somewhat more than $k_{cat}/K_m(O_2)$, but it

cannot account for the greatly decreased value for k_5 and the elevated kinetic isotope effects. Interestingly, there are other residues near the Cu_H site that affect steps in the mechanism between formation of the ternary complex and product release. Mutation of Y79W, less than 5 Å away from Cu_H, shows a decrease in k_{cat} by approximately 200-fold (*13*).

A second possibility is that O_2 activation and substrate hydroxylation occur at the Cu_H site. A large volume of evidence suggests otherwise (*21*, *33*, *39*). Substrate-induced CO binding to the Cu_H site has implicated it as a possible O_2 binding site (*9*), with a suggested role for His^{172} as an active site acid catalyst (*10*). This mechanism would require that O_2 first bind to the Cu_H site, receiving a proton and electron, and then channel across the water-filled cavity to Cu_M. However, as noted above, full coupling of O_2 consumption with hydroxylated product formation (Table 1) rules out a superoxide channeling mechanism and suggests that no drastic changes have occurred at the active site to perturb the mechanism of O_2 activation. The only alternative would be for substrate to move from its crystallographically defined binding site adjacent to the Cu_M, similar to a mechanism proposed in ref *13*.

A third possibility is that H172A induces subtle but critical changes to the protein backbone and to a hydrogen-bonding network linking the copper sites. Earlier studies have indicated that mutation of a ligand to Cu_M (M314) produces long-range structural perturbations to the Cu_H site (*40*). In the crystal structures of oxidized and reduced PHMcc, with and without bound substrate, there appears to be a water molecule in close proximity and hydrogen bonded to H108. On the basis of the X-ray structure shown in Figure 1, a hydrogen bond between H108 and substrate may be expected to be important in maintaining the substrate in its proper orientation for C−H cleavage. The large reduction in the H-transfer rate for H172A may reflect an impact of a second Cu_H ligand on this H-bonded network. Quantum mechanical tunneling has been shown to play a central role in the transfer of hydrogen from substrate to the activated O_2 species in WT PHM (*53*). Emerging models for tunneling in enzyme reactions invoke the participation of two types of protein motions to achieve effective wave function overlap between the hydrogen donor and acceptor (*54*). The first involves a sampling of a large number of protein configurations, with only a small subset of these configurations being optimal for tunneling (termed protein preorganization). We note that the recent snapshot of the PHM active site, Figure 1, indicates that the substrate and O_2 are not optimally positioned in relation to each other for tunneling to occur, with the likely participation of a dynamical sampling of protein configurations to bring the two substrates into the correct orientation for catalysis. Once the optimal configurations have been reached, additional heavy atom motions are invoked to affect the relative energy levels and distance between the reactants [λ and Δr, respectively, referred to collectively as the reorganization terms (*55*)]. Disruption of the critical H-bonded network in PHM may be expected to affect both the preorganization and reorganization barriers, leading to a reduced rate for H-transfer and, possibly, altered parameters for the tunneling process. While the former effect is clearly demonstrated herein, the impact of H172A on the tunneling parameters (in particular, the temperature dependence of the intrinsic isotope effect) will be the focus at future studies.

CONCLUSIONS

Residue His^{172} has been found to play a very important role in the mechanism of PHM. As a ligand of Cu_H, its absence does not appear to have a significant effect on copper binding. However, deletion of this residue results in a 12000-fold decrease in the hydrogen transfer step with smaller effects on substrate binding and electron transfer/product release steps (400−2000-fold, respectively). One possible consequence of H172 removal on the mechanism of substrate hydroxylation may be a nonspecific structural change to the entire protein that creates a suboptimal conformation of active protein that reduces the values for all rate constants by a similar value. An additional effect must be invoked to explain the fact that H172A has its greatest impact on H-transfer. A disruption of a hydrogen-bonded network through the water-filled cavity connecting the two copper sites is postulated to interfere with the preorganization and subsequent reorganization that promotes effective hydrogen wave function overlap and transfer of the hydrogen from the α-carbon of substrate to the activated Cu_M oxygen species.

ACKNOWLEDGMENT

We thank Prof. Betty Eipper (DK32949) and Dr. Joseph Bell for providing some of the enzyme samples and for advice on purification procedures.

REFERENCES

1. Klinman, J. P. (1996) Mechanisms whereby mononuclear copper proteins functionalize organic substrates, *Chem. Rev. 96*, 2541−2561.
2. Prigge, S. T., Mains, R. E., Eipper, B. A., and Amzel, L. M. (2000) New insights into copper monooxygenases and peptide amidation: structure, mechanism and function, *Cell. Mol. Life Sci. 57*, 1236−1259.
3. Brenner, M. C., Murray, C. J., and Klinman, J. P. (1989) Rapid freeze- and chemical-quench studies of dopamine beta-monooxygenase: comparison of pre-steady-state and steady-state parameters, *Biochemistry 28*, 4656−4664.
4. Freeman, J. C., Villafranca, J. J., and Merkler, D. J. (1993) Redox cycling of enzyme-bound copper during peptide amidation, *J. Am. Chem. Soc. 115*, 4923−4924.
5. Fitzpatrick, P. F., and Villafranca, J. J. (1985) Mechanism-based inhibitors of dopamine beta-hydroxylase containing acetylenic or cyclopropyl groups, *J. Am. Chem. Soc. 107*, 5022−5023.
6. Fitzpatrick, P. F., Flory, D. R., Jr., and Villafranca, J. J. (1985) 3-Phenylpropenes as mechanism-based inhibitors of dopamine beta-hydroxylase: evidence for a radical mechanism, *Biochemistry 24*, 2108−2114.
7. Miller, S. M., and Klinman, J. P. (1985) Secondary isotope effects and structure-reactivity correlations in the dopamine beta-monooxygenase reaction: evidence for a chemical mechanism, *Biochemistry 24*, 2114−2127.
8. Wimalasena, K., and May, S. W. (1989) Dopamine beta-monooxygenase catalyzed aromatization of 1-(2-aminoethyl)-1,4-cyclohexadiene—redirection of specificity and evidence for a hydrogen-atom transfer mechanism, *J. Am. Chem. Soc. 111*, 2729−2731.
9. Jaron, S., and Blackburn, N. J. (1999) Does superoxide channel between the copper centers in peptidylglycine monooxygenase? A new mechanism based on carbon monoxide reactivity, *Biochemistry 38*, 15086−15096.
10. Jaron, S., Mains, R. E., Eipper, B. A., and Blackburn, N. J. (2002) The catalytic role of the copper ligand H172 of peptidylglycine alpha-hydroxylating monooxygenase (PHM): a spectroscopic study of the H172A mutant, *Biochemistry 41*, 13274−13282.
11. Prigge, S. T., Kolhekar, A. S., Eipper, B. A., Mains, R. E., and Amzel, L. M. (1999) Substrate-mediated electron transfer in peptidylglycine alpha-hydroxylating monooxygenase, *Nat. Struct. Biol. 6*, 976−983.

12. Prigge, S. T., Eipper, B. A., Mains, R. E., and Amzel, L. M. (2004) Dioxygen binds end-on to mononuclear copper in a pre-catalytic enzyme complex, *Science 304*, 864−867.
13. Bell, J., El Meskini, R., D'Amato, D., Mains, R. E., and Eipper, B. A. (2003) Mechanistic investigation of peptidylglycine alpha-hydroxylating monooxygenase via intrinsic tryptophan fluorescence and mutagenesis, *Biochemistry 42*, 7133−7142.
14. Owen, T. C., and Merkler, D. J. (2004) A new proposal for the mechanism of glycine hydroxylation as catalyzed by peptidylglycine alpha-hydroxylating monooxygenase (PHM), *Med. Hypotheses 62*, 392−400.
15. Evans, J. P., Ahn, K., and Klinman, J. P. (2003) Evidence that dioxygen and substrate activation are tightly coupled in dopamine beta-monooxygenase. Implications for the reactive oxygen species, *J. Biol. Chem. 278*, 49691−49698.
16. Klinman, J. P. (2006) The copper-enzyme family of dopamine beta-monooxygenase and peptidylglycine alpha-hydroxylating monooxygenase: resolving the chemical pathway for substrate hydroxylation, *J. Biol. Chem. 281*, 3013−3016.
17. Chen, P., and Solomon, E. I. (2004) Oxygen activation by the noncoupled binuclear copper site in peptidylglycine alpha-hydroxylating monooxygenase. Reaction mechanism and role of the noncoupled nature of the active site, *J. Am. Chem. Soc. 126*, 4991−5000.
18. Blackburn, N. J., Rhames, F. C., Ralle, M., and Jaron, S. (2000) Major changes in copper coordination accompany reduction of peptidylglycine monooxygenase: implications for electron transfer and the catalytic mechanism, *J. Biol. Inorg. Chem. 5*, 341−353.
19. Francisco, W. A., Merkler, D. J., Blackburn, N. J., and Klinman, J. P. (1998) Kinetic mechanism and intrinsic isotope effects for the peptidylglycine alpha-amidating enzyme reaction, *Biochemistry 37*, 8244−8252.
20. Kolhekar, A. S., Keutmann, H. T., Mains, R. E., Quon, A. S. W., and Eipper, B. A. (1997) Peptidylglycine alpha-hydroxylating monooxygenase: active site residues, disulfide linkages, and a two-domain model of the catalytic core, *Biochemistry 36*, 10901−10909.
21. Boswell, J. S., Reedy, B. J., Kulathila, R., Merkler, D., and Blackburn, N. J. (1996) Structural investigations on the coordination environment of the active-site copper centers of recombinant bifunctional peptidylglycine alpha-amidating enzymes, *Biochemistry 35*, 12241−12250.
22. Merkler, D. J., Kulathila, R., Tamburini, P. P., and Young, S. D. (1992) Selective inactivation of the hydroxylase-activity of bifunctional rat peptidylglycine alpha-amidating enzyme, *Arch. Biochem. Biophys. 294*, 594−602.
23. Wittaker, J. W., Orville, A. M., and Lipscomb, J. D. (1990) Protocatechuate 3, 4-dioxygenase from *Brevibacterium fuscum*, *Methods Enzymol. 188*, 82−88.
24. Bundgaard, H., and Kahns, A. H. (1991) Chemical-stability and plasma-catalyzed dealkylation of peptidyl alpha-hydroxyglycine derivatives—intermediates in peptide alpha-amidation, *Peptides 12*, 745−748.
25. Mounier, C. E., Shi, J., Sirimanne, S. R., Chen, B. H., Moore, A. B., GillWoznichak, M. M., Ping, D. S., and May, S. W. (1997) Pyruvate-extended amino acid derivatives as highly potent inhibitors of carboxyl-terminal peptide amidation, *J. Biol. Chem. 272*, 5016−5023.
26. Cleland, W. W. (1979) Statistical analysis of enzyme kinetic data, *Methods Enzymol. 63*, 103−138.
27. Khan, M. M. T., and Martell, A. E. (1967) Metal ion and metal chelate catalyzed oxidation of ascorbic acid by molecular oxygen. I. Cupric and ferric ion catalyzed oxidation, *J. Am. Chem. Soc. 89*, 4176−4185.
28. Miller, D. M., Buettner, G. R., and Aust, S. D. (1990) Transition-metals as catalysts of autoxidation reactions, *Free Radical Biol. Med. 8*, 95−108.
29. Kulathila, R., Consalvo, A. P., Fitzpatrick, P. F., Freeman, J. C., Snyder, L. M., Villafranca, J. J., and Merkler, D. J. (1994) Bifunctional peptidylglycine alpha-amidating enzyme requires 2 copper atoms for maximum activity, *Arch. Biochem. Biophys. 311*, 191−195.
30. Stewart, L. C., and Klinman, J. P. (1987) Characterization of alternate reductant binding and electron-transfer in the dopamine beta-monooxygenase reaction, *Biochemistry 26*, 5302−5309.
31. Kizer, J. S., Bateman, R. C., Miller, C. R., Humm, J., Busby, W. H., and Youngblood, W. W. (1986) Purification and characterization of a peptidylglycine monooxygenase from porcine pituitary, *Endocrinology 118*, 2262−2267.
32. Cook, P. F., and Cleland, W. W. (1981) Mechanistic deductions from isotope effects in multireactant enzyme mechanisms, *Biochemistry 20*, 1790−1796.
33. Reedy, B. J., and Blackburn, N. J. (1994) Preparation and characterization of half-apo dopamine beta-hydroxylase by selective removal of CuA. Identification of a sulfur ligand at the dioxygen binding-site by EXAFS and FTIR spectroscopy, *J. Am. Chem. Soc. 116*, 1924−1931.
34. Jaron, S., and Blackburn, N. J. (2001) Characterization of a half-apo derivative of peptidylglycine monooxygenase. Insight into the reactivity of each active site copper, *Biochemistry 40*, 6867−6875.
35. Tian, G., Berry, J. A., and Klinman, J. P. (1994) Oxygen-18 kinetic isotope effects in the dopamine beta-monooxygenase reaction: evidence for a new chemical mechanism in non-heme metallomonooxygenases, *Biochemistry 33*, 226−234 [erratum: (1994) *Biochemistry 33*, 14650].
36. Francisco, W. A., Blackburn, N. J., and Klinman, J. P. (2003) Oxygen and hydrogen isotope effects in an active site tyrosine to phenylalanine mutant of peptidylglycine alpha-hydroxylating monooxygenase: mechanistic implications, *Biochemistry 42*, 1813−1819.
37. Eipper, B. A., Quon, A. S. W., Mains, R. E., Boswell, J. S., and Blackburn, N. J. (1995) The catalytic core of peptidylglycine alpha-hydroxylating monooxygenase—Investigation by site-directed mutagenesis, Cu X-ray-absorption spectroscopy, and electron-paramagnetic-resonance, *Biochemistry 34*, 2857−2865.
38. Yonekura, H., Anzai, T., Kato, I., Furuya, Y., Shizuta, S., Takasawa, S., and Okamoto, H. (1996) Identification of the five essential histidine residues for peptidylglycine monooxygenase, *Biochem. Biophys. Res. Commun. 218*, 495−499.
39. Prigge, S. T., Kolhekar, A. S., Eipper, B. A., Mains, R. E., and Amzel, L. M. (1997) Amidation of bioactive peptides: the structure of peptidylglycine alpha-hydroxylating monooxygenase, *Science 278*, 1300−1305.
40. Siebert, X., Eipper, B. A., Mains, R. E., Prigge, S. T., Blackburn, N. J., and Amzel, M. L. (2005) The catalytic copper of peptidylglycine-a-hydroxylating monooxygenase also plays a critical structural role, *Biophys. J. 89*, 3312−3319.
41. Maryniak, D. M., Kadkhodayan, S., Crull, G. B., Bryson, T. A., and Dawson, J. H. (1993) The synthesis of 1R- and 1S-5-methylenylcamphor and their epoxidation by cytochrome P450-cam, *Tetrahedron 49*, 9373−9384.
42. Kadkhodayan, S., Coulter, E. D., Maryniak, D. M., Bryson, T. A., and Dawson, J. H. (1995) Uncoupling oxygen transfer and electron transfer in the oxygenation of camphor analogues by cytochrome P450-CAM: direct observation of an intermolecular isotope effect for substrate C−H activation, *J. Biol. Chem. 270*, 28042−28048.
43. Loida, P. J., and Sligar, S. G. (1993) Engineering cytochrome P450-cam to increase the stereospecificity and coupling of aliphatic hydroxylation, *Protein Eng. 6*, 207−212.
44. Loida, P. J., and Sligar, S. G. (1993) Molecular recognition in cytochrome P450: mechanism for the control of uncoupling reactions, *Biochemistry 32*, 11530−11538.
45. Yeom, H. Y., and Sligar, S. G. (1997) Oxygen activation by cytochrome P450(BM-3): effects of mutating an active site acidic residue, *Arch. Biochem. Biophys. 337*, 209−216.
46. Kemsley, J. N., Wasinger, E. C., Datta, S., Mitic, N., Acharya, T., Hedman, B., Caradonna, J. P., Hodgson, K. O., and Solomon, E. I. (2003) Spectroscopic and kinetic studies of PKU-inducing mutants of phenylalanine hydroxylase: Arg158Gln and Glu280Lys, *J. Am. Chem. Soc. 125*, 5677−5686.
47. Sternson, A. W., McCreery, R., Feinberg, B., and Adams, R. N. (1973) Electrochemical studies of adrenergic neurotransmitters and related compounds, *J. Electroanal. Chem. 46*, 313−321.
48. Iyanagi, T., Yamazaki, I., and Anan, K. F. (1985) One-electron oxidation-reduction properties of ascorbic-acid, *Biochim. Biophys. Acta 806*, 255−261.
49. Ljones, T., and Flatmark, T. (1974) Dopamine beta-hydroxylase—Evidence against a ping-pong mechanism, *FEBS Lett. 49*, 49−52.
50. Rosenberg, R. C., Gimble, J. M., and Lovenberg, W. (1980) Inhibition of dopamine beta-hydroxylase by alternative electron-donors, *Biochim. Biophys. Acta 613*, 62−72.
51. Fitzpatrick, P. F., Harpel, M. R., and Villafranca, J. J. (1986) Use of alternate substrates to probe the order of substrate addition to dopamine beta-hydroxylase, *Arch. Biochem. Biophys. 249*, 70−75.

52. Ahn, N., and Klinman, J. P. (1983) Mechanism of modulation of dopamine beta-monooxygenase by pH and fumarate as deduced from initial rate and primary deuterium isotope effect studies, *Biochemistry 22*, 3096−3106.
53. Francisco, W. A., Knapp, M. J., Blackburn, N. J., and Klinman, J. P. (2002) Hydrogen tunneling in peptidylglycine alpha-hydroxylating monooxygenase, *J. Am. Chem. Soc. 124*, 8194−8195.
54. Nagel, Z. D., and Klinman, J. P. (2006) Tunneling and dynamics in enzymatic hydride transfer, *Chem. Rev. 106*, 3095−3118.
55. Knapp, M. J., Rickert, K., and Klinman, J. P. (2002) Temperature-dependent isotope effects in soybean lipoxygenase-1: correlating hydrogen tunneling with protein dynamics, *J. Am. Chem. Soc. 124*, 3865−3874.
56. Palcic, M. M., and Klinman, J. P. (1983) Isotopic probes yield microscopic constants—Separation of binding-energy from catalytic efficiency in the bovine plasma amine oxidase reaction, *Biochemistry 22*, 5957−5966.

BI061734C